

Effect of KNL1 on the proliferation and apoptosis of colorectal cancer cells

Technology in Cancer Research & Treatment
Volume 18: 1-12
© The Author(s) 2019
Article reuse guidelines:
sagepub.com/journals-permissions
DOI: 10.1177/1533033819858668
journals.sagepub.com/home/tct



Tianliang Bai, PhD^{1,2}, Yalei Zhao, PhD¹, Yabin Liu, PhD¹, Bindan Cai, MB³, Ning Dong, MB⁴, and Binghui Li, PhD¹

Abstract

Objective: To identify the expression of kinetochore scaffold I (*KNL1*) in colorectal tumor tissues and to clarify the role of this gene in the proliferation capability of colorectal cancer cells. **Methods:** A total of 108 paired colorectal tumor and normal tissue samples were collected from patients with colorectal cancer and subjected to quantitative polymerase chain reaction and immunohistochemistry analyses. Expression levels of *KNL1* mRNA and protein were compared between tumor and normal tissues, and *KNL1* levels were evaluated in relation to the patients' tumor differentiation, sex, lymph node metastasis, TNM stage, infiltration depth, age, and tumor location. Survival curves were also constructed and compared between patients with tumor samples with and without *KNL1* protein expression. *KNL1* was under-expressed in colorectal cancer cells *in vitro* using lentiviral transfection with short hairpin RNA, and its function was evaluated by proliferation, colony-formation, and apoptosis assays. Expression levels of BUB1 protein were also compared between tumor and normal tissues, and the correlation between *KNL1* expression and BUB1 expression in colorectal cancer tissues was examined. **Results:** *KNL1* mRNA and protein were both highly expressed in colorectal tumor tissues compared with paired normal tissues. *KNL1* downregulation significantly inhibited colorectal cancer cell proliferation and colony formation, and promoted apoptosis. *KNL1* protein expression was significantly associated with tumor differentiation, but not with sex, lymph node metastasis, TNM stage, infiltration depth, age, or tumor location. *KNL1* protein expression was also significantly associated with poorer survival. Moreover, there was a significant correlation between *KNL1* and BUB1 in colorectal cancer tissues. **Conclusions:** *KNL1* plays an effective role in decreasing apoptosis and promoting the proliferation of colorectal cancer cells, suggesting that its inhibition may represent a promising therapeutic approach in patients with colorectal cancer.

Keywords

Kinetochore scaffold I, *KNL1*, colorectal tumor, cell growth, prognosis, gene expression, protein expression

Abbreviations

BUB, budding uninhibited by benzimidazoles; CRC, colorectal carcinoma; FACS, fluorescence-activated cell sorting; GAPDH, glyceraldehyde 3-phosphate dehydrogenase; GSEA, gene set enrichment analysis; *KNL1*, kinetochore scaffold I; KNM, *KNL1*/MIS12/NDC80; MCPH, primary microcephaly; MTT, methyl-thiazol-tetrazolium; PBS, phosphate-buffered saline; qRT-PCR, quantitative reverse transcription-polymerase chain reaction; shCtrl, control short hairpin RNA; sh*KNL1*, *KNL1* short hairpin RNA; TCGA, The Cancer Genome Atlas

Received: December 28, 2018; Revised: April 14, 2019; Accepted: May 22, 2019.

¹ Department of General Surgery, Hebei Medical University Fourth Affiliated Hospital (Hebei Provincial Tumor Hospital), Shijiazhuang, Hebei, P.R. China

² Department of Gastrointestinal Surgery, Affiliated Hospital of Hebei University, Baoding, Hebei, P.R. China

³ Department of Neurology, Zhuozhou City Hospital, Zhuozhou, Hebei, P.R. China

⁴ Department of Radiology, Zhuozhou City Hospital, Zhuozhou, Hebei, P.R. China

Corresponding Author:

Binghui Li, PhD, Department of General Surgery, Hebei Medical University Fourth Affiliated Hospital (Hebei Provincial Tumor Hospital), 12 Jiankang Road, Shijiazhuang, Hebei 050011, P.R. China.

Email: nanion@163.com



Creative Commons Non Commercial CC BY-NC: This article is distributed under the terms of the Creative Commons Attribution-NonCommercial 4.0 License (<http://www.creativecommons.org/licenses/by-nc/4.0/>) which permits non-commercial use, reproduction and distribution of the work without further permission provided the original work is attributed as specified on the SAGE and Open Access pages (<https://us.sagepub.com/en-us/nam/open-access-at-sage>).

Introduction

Colorectal carcinoma (CRC) has been reported to be the second deadliest cancer.¹⁻⁴ Although the overall morbidity and mortality of CRC have decreased in recent decades, there has been a considerable increase in patients <50 years of age.⁴⁻⁶ Additionally, the tumor is often not completely resectable with a 5-year survival rate of only 14%,^{5,6} and despite advances in therapeutic strategies and diagnostic approaches, the prognoses for patients with CRC typically remain poor.⁷ There is thus an urgent need to develop new treatment approaches for CRC.

We previously reported the effects of cloning *D40* on chromosome 15.⁸ *D40* and *BUB1* (budding uninhibited by benzimidazoles 1) were characterized as cancer-related genes primarily expressed in the testis under normal conditions, but which were also widely expressed in primary tumors of various origins and in assorted cancer cell lines.⁹⁻¹⁶ *AF15q14*, a human gene on chromosome 15, was shown to be identical to the *D40* gene,⁸ and a previous study reported the mutual translocation of *AF15q14* with the mixed lineage leukemia gene *MLL* in acute myeloid leukemia.¹⁷ Furthermore, *D40* expression has been reported to be associated with pathological features of primary lung tumors, such as the degree of differentiation and the patient's smoking history.¹⁰ In a study of human testes, *D40* was found to be expressed in pre-acrosomes and spermatocytes.¹⁸ A follow-up study revealed that blinkin, a type of kinetochore protein in the mitotic machinery, was identical to kinetochore scaffold 1 (KNL1).¹⁹ In addition to binding with Ndc80 and Mis12 complexes to create the KNL1, MIS12, NDC80 (KMN) network, KNL1/blinkin also bound to other proteins, including tubulin, the spindle assembly checkpoint (SAC) proteins BUBR1 and BUB1, and protein phosphatase 1.¹⁹⁻²³ Such binding suggests that KNL1/blinkin and BUB1 may have crucial impacts on kinetochore formation in terms of the connection between spindles and chromosomes, as well as regulation of the SAC.¹⁹⁻²⁸

Primary microcephaly (MCPH) is a rare congenital neurodevelopmental disorder with autosomal recessive features.^{29,30} Patients with MCPH have a smaller head circumference and smaller brains, leading to varying levels of mental retardation. However, patients with MCPH generally do not have any additional somatic or neurological disorders. MCPH is a genetically heterogeneous condition controlled by several chromosomal loci.²⁹ Previous studies identified an MCPH locus on chromosome 15,³⁰ and the gene responsible was identified as *CASC5*, which is identical to *KNL1*.³¹ Brain development requires rapid cell division, thus suggesting that *KNL1* may play a significant role in *in vivo* cell division.

As noted above,^{8,10,17,19,22} there are several different names for the same gene/protein (KNL1, AF15q14, KIAA1570, *CASC5*, blinkin, D40) and we have therefore used the term KNL1 throughout the present study.

In the present study, we analyzed KNL1 gene and protein expression levels in CRC and matched adjacent noncancerous tissues and in CRC cell lines. We also examined the effect of *KNL1* knockdown on CRC cell growth *in vitro* by transfecting

RKO and HT-29 CRC cell lines with short hairpin KNL1 RNA (shKNL1).

Materials and Methods

Bioinformatics analysis

Gene expression data were obtained from The Cancer Genome Atlas website (TCGA, <https://tcga-data.nci.nih.gov/tcga/>) in relation to the colon adenocarcinoma (COAD) project. In the COAD project, gene set enrichment analysis (GSEA) was carried out to gain further insights into the biological pathways involved in the pathogenesis of CRC. GSEA provides a method for analyzing and interpreting microarray data in relation to biological states.³²

Patients and samples

We collected CRC and paired adjacent noncancerous tissue samples from 108 patients with colorectal cancer at the Department of General Surgery of the Fourth Hospital of Hebei Medical University (Shijiazhuang, Hebei, China). Intraoperative colorectal cancer tissues and adjacent normal tissues >10 cm away from colorectal cancer tissues were studied. All patients were diagnosed for the first time and had undergone no other treatments such as radiotherapy, chemotherapy, or immunotherapy before surgery. All experiments were approved by the Ethics Committee of the Fourth Hospital of Hebei Medical University, and all clinical investigations were conducted according to the principles expressed in the Declaration of Helsinki. All patients provided written informed consent for participation in this study. All patients underwent outpatient review and telephone follow-up to obtain information on postoperative survival status, quality of life, tumor differentiation, sex, lymph node metastasis, TNM stage, infiltration depth, age, tumor location, and imaging findings. Survival time was determined from the date of initial diagnosis to the date of last postoperative follow-up or death. Postoperative staging was performed according to the American Joint Committee on Cancer Seventh Edition staging method.

Cell lines and cell culture

Human CRC (SW480, HT-29, HCT-116, and RKO) and normal colonic epithelial cell lines (NCM460) were purchased from the American Type Culture Collection (Manassas, VA, USA). Cells were maintained in RPMI-1640 (Gibco; Thermo Fisher Scientific, Inc., Waltham, MA, USA) supplemented with 10% fetal bovine serum (Gibco; Thermo Fisher Scientific, Inc.) in a humidified atmosphere containing 5% CO₂ at 37°C.

Immunohistochemistry

Immunohistochemistry was carried out using the streptavidin-biotin-peroxidase method according to the manufacturer's protocol (LSAB Universal Kit; DAKO Corporation, Carpinteria, CA, USA). The sections were deparaffinized by xylene and dehydrated in graded ethanol, followed by antigen retrieval in a steam pressure cooker. The sections were treated in 3%

hydrogen peroxide in phosphate-buffered saline (PBS) for 15 minutes and then rinsed in PBS. The sections were placed in 500 mL of 0.01 M citric acid-buffered solution (pH 7.0) and microwaved at 500 W for 5 minutes. After thorough washing, the sections were incubated with normal rabbit serum for 20 minutes at room temperature to avoid nonspecific binding of the antibodies. Endogenous peroxidase activity was inhibited by incubation with 0.3% hydrogen peroxide in methanol. After blocking nonspecific binding, the sections were incubated overnight with antibodies against BUB1 and KNL1 (dilution, 1:300; Biorbyt Ltd., Cambridge, UK). Sections were then incubated with streptavidin peroxidase complex, developed with 3,3'-diaminobenzidine solution, counterstained with Mayer's/Lillie Mayer's hematoxylin, and mounted.

Evaluation of KNL1 and BUB1 protein expression

The immunostained specimens were evaluated independently by two observers (authors Y.B. Liu and B.H. Li) with no knowledge of the clinicopathological data. In the event of a discrepancy, a consensus was reached following additional assessment. The staining intensity of cancer cells was graded on a 4-point scale: 0 = no staining, 1 = weak staining, 2 = moderate staining, and 3 = strong staining. The percentage of stained cancer cells was also graded on a 4-point scale: 0 = no cells, 1 = <10%, 2 = 10% to 50%, and 3 = >50%. The intensity score was multiplied by the percentage score to obtain an overall score.

RNA extraction and reverse transcription-quantitative polymerase chain reaction (RT-qPCR)

Whole RNA was extracted from the sampled cells and tissues using TRIzol[®] reagent (Invitrogen; Thermo Fisher Scientific, Inc.). cDNA was generated by RT using M-MLV Reverse Transcriptase (Promega Corp., Madison, WI, USA) according to the manufacturer's protocol. A total of 1 μ L cDNA was used as the template for qPCR. Glyceraldehyde 3-phosphate dehydrogenase (GAPDH) was used as an internal control. The primer sequences were as follows: *KNL1*, forward 5'-ACA TTG GAA AAA GCG CAA GTTG-3' and reverse 5'-TTG CAC TGG GCA ATA ATT GGC-3'; *GAPDH*, forward 5'-TGA CTT CAA CAG CGA CAC CCA-3' and reverse 5'-CAC CCT GTT GCT GTA GCC AAA-3'. Thermocycling comprised initial denaturation at 95°C for 30 s followed by 45 cycles of denaturation at 95°C for 5 s and extension at 60°C for 30 s. Each experiment was performed in triplicate and relative quantitative gene expression was calculated as described previously.³³

Western blotting

Cells and tissues were lysed using RIPA buffer (Thermo Fisher Scientific, Inc.). Lysates were electrophoresed by 10% sodium dodecyl sulfate-polyacrylamide gel electrophoresis (Thermo Fisher Scientific, Inc.) and transferred onto polyvinylidene difluoride membranes (Thermo Fisher Scientific, Inc.). After blocking for 1 hour in 5% skimmed milk, the membranes were

incubated overnight at 4°C with rabbit antibodies against KNL1 (dilution, 1:500; Biorbyt Ltd.) and GAPDH (dilution, 1:800; Santa Cruz Biotechnology, Inc., Dallas, TX, USA), washed four times in TBST, and then incubated at room temperature for 1 hour with a horseradish peroxidase-conjugated secondary antibody (dilution, 1:10,000; catalog no., 323-065-021; Jackson ImmunoResearch, Inc., West Grove, PA, USA). Protein bands were visualized using a chemiluminescence system (Thermo Fisher Scientific, Inc.) according to the manufacturer's protocol. The band intensities were quantified using Image-Quant Software v3.0 (LI-COR Biosciences, Lincoln, NE, USA). This experiment was repeated in triplicate.

Construction of recombinant lentiviral vector and cell transduction

KNL1 shRNA (shKNL1) and control shRNA (shCtrl) were designed by GeneChem Co., Ltd. (Shanghai, China) from the unabridged sequence of *D40/KNL1*, which is targeted at the human *KNL1* gene (GenBank no. NM_144508). The targeting sequence of *KNL1* was 5'-CAG AGT TGT ATG GTG GAAA-3'. The efficiency of *KNL1* knockdown was tested following synthesis and insertion of stem-loop oligonucleotides into a lentivirus-based pGV115-GFP vector (GeneChem Co. Ltd.) with AgeI/EcoRI sites. Lentivirus particles were prepared as described previously.³⁴ RKO and HT-29 cells (2×10^5 cells/well) were cultured in 6-well plates and transfected with either negative control (shCtrl) lentivirus or *KNL1* (shKNL1) lentivirus at a multiplicity of infection of 5. A blank control group (uninfected) was set up simultaneously. Cells were incubated for 5 days at 37°C in an atmosphere containing 5% CO₂. After 72 hours of transfection, cells were observed using a fluorescence microscope (IX71; Olympus Corp., Tokyo, Japan). The knockdown efficiency was measured after 5 days using western blotting and RT-qPCR.

Cell growth assay

ShKNL1-transfected, shCtrl-transfected, and blank control RKO and HT-29 cells in logarithmic growth phase were cultured in 96-well plates at a density of 2,000 cells/well for 5 days at 37°C in an atmosphere containing 5% CO₂. Cell numbers were recorded every day using a Celigo Imaging Cytometer (Nexcelom Bioscience, Lawrence, MA, USA). All assays were performed in triplicate.

Methyl-thiazol-tetrazolium (MTT) assay

ShKNL1-transfected, shCtrl-transfected, and blank control RKO and HT-29 cells were seeded and cultured in 96-well plates at a density of 2,000 cells/well at 37°C and their proliferation was assessed each day for 5 days. Briefly, 20 μ L MTT (5 mg/mL; Genview, Craigie Burn, Australia) was added to each well and incubated at 37°C for 4 hours. The culture medium was removed and 100 μ L of dimethyl sulfoxide was added to each well to dissolve the crystals. Plates were agitated for 2 to 5 minutes and the absorbance at 490 nm was read using

a microplate reader (Tecan Infinite, Tecan GmbH, Austria). All experiments were performed in triplicate.

Colony-formation assay

Cells transfected with shKNL1 or shCtrl vectors in logarithmic growth phase were re-suspended in RPMI-1640 and seeded in 6-well plates at a density of 800 cells/well and then incubated for 14 days. Cell colonies were then observed by fluorescence microscopy (IX71; Olympus Corp.). Cells were fixed with paraformaldehyde (1 mL/well; Sangon Biotech Co. Ltd., Shanghai, China) for 30 minutes, washed with phosphate-buffered saline (PBS), and then stained with 500 μ L 0.5% crystal violet (Sangon Biotech Co. Ltd.) for 5 minutes. The stained cells were then washed with ddH₂O and dried at room temperature. Finally, cell colonies were observed under a microscope (Cai Kang Optical Instrument Co., Ltd, Shanghai, China). All experiments were performed in triplicate.

Fluorescence-activated cell sorting (FACS)

FACS was used to analyze cell apoptosis.³⁵ In brief, RKO cells transfected with shCtrl or shKNL1 were seeded in 6-well plates for 120 hours and grown to 70% confluence, harvested, and washed with 1 \times binding buffer, followed by the addition of 10 μ L of Annexin V-allophycocyanin Detection kit (eBioscience; Thermo Fisher Scientific, Inc.) per 200 μ L of the adjusted suspension for 15 minutes in the dark at room temperature. Flow cytometry analysis was carried out after cell staining. All experiments were performed in triplicate.

Cell cycle detection

Cells collected from each group were washed in cold PBS and then adjusted to a concentration of 1 \times 10⁶ cells/mL. The cells were then fixed with 70% ethyl alcohol overnight, incubated with RNaseA at 37°C in a water bath for 30 minutes, followed by staining with propidium iodide at 4°C for 30 minutes. The DNA content was measured by flow cytometry.

Statistical analysis

Statistical analyses were carried out using IBM SPSS Statistics for Windows, Version 19.0 (IBM Corp., Armonk, NY, USA). All data are presented as the mean \pm standard deviation. Comparisons between two groups were made using Student's *t*-test, and correlations between KNL1 expression and clinicopathological parameters were analyzed by the χ^2 test. Survival curves were plotted using the log-rank (Mantel-Cox) test and the Gehan-Breslow-Wilcoxon test. A value of *P*<0.05 was considered to indicate a significant difference.

Results

Demographics

The patients' demographic information is presented in Table 1.

Table 1. Patients' demographic information.

| Clinical parameters | Patients, n |
|----------------------|-------------|
| Age (years) | |
| <60 | 42 |
| \geq 60 | 66 |
| Sex | |
| Male | 63 |
| Female | 45 |
| Differentiation | |
| Level I-II | 48 |
| Level III | 60 |
| TNM stage | |
| I-II | 69 |
| III | 39 |
| Lymphatic metastasis | |
| No | 66 |
| Yes | 42 |
| Infiltration depth | |
| T1-T2 | 30 |
| T3-T4 | 78 |
| Tumor location | |
| Colon | 42 |
| Rectum | 66 |

Expression of KNL1 and BUB1 in normal and CRC tissues

KNL1 gene and protein expression levels in CRC and paracancerous tissues were measured by RT-qPCR and western blot, respectively. The PCR products for *GAPDH* and *KNL1* were 121 and 213 base pairs in length, respectively. KNL1 mRNA and protein levels were both significantly higher in CRC compared with normal tissues (*P*<0.05) (Figure 1A and B).

Immunohistochemical analysis of serial sections of 108 CRC samples showed that KNL1 and BUB1 proteins were located mainly in the nucleus of the same cancer cells (Figure 1C-F). KNL1 mRNA expression levels were also significantly higher in CRC compared with normal tissues in COAD gene expression data collected from the TCGA website (<https://tcga-data.nci.nih.gov/tcga/>) (*P*<0.001) (Figure 1G). The calculated regression coefficient between the expression scores of KNL1 and BUB1 showed a significant correlation between KNL1 and BUB1 expression in CRC (*P*<0.0001) (Figure 1H). However, KNL1 and BUB1 were hardly expressed in adjacent normal tissues (Figure 1I and J).

The mean overall scores for KNL1 and BUB1 in the 108 tumors were 4.9 and 5.4, respectively, and these were therefore used as the mean overall cut-off scores for discriminating KNL1 and BUB1 protein expression statuses, respectively. Samples with a KNL1 score >4.9 were considered as KNL1-positive and samples with a score \leq 4.9 were considered KNL1-negative. Samples with a BUB1 score >5.4 were considered BUB1-positive and samples with a score \leq 5.4 were considered BUB1-negative.

To explore the medical significance of KNL1 expression in CRC, we analyzed its expression in relation to various clinicopathological characteristics. Among the 108 patients, KNL1 expression in tumor specimens was substantially associated

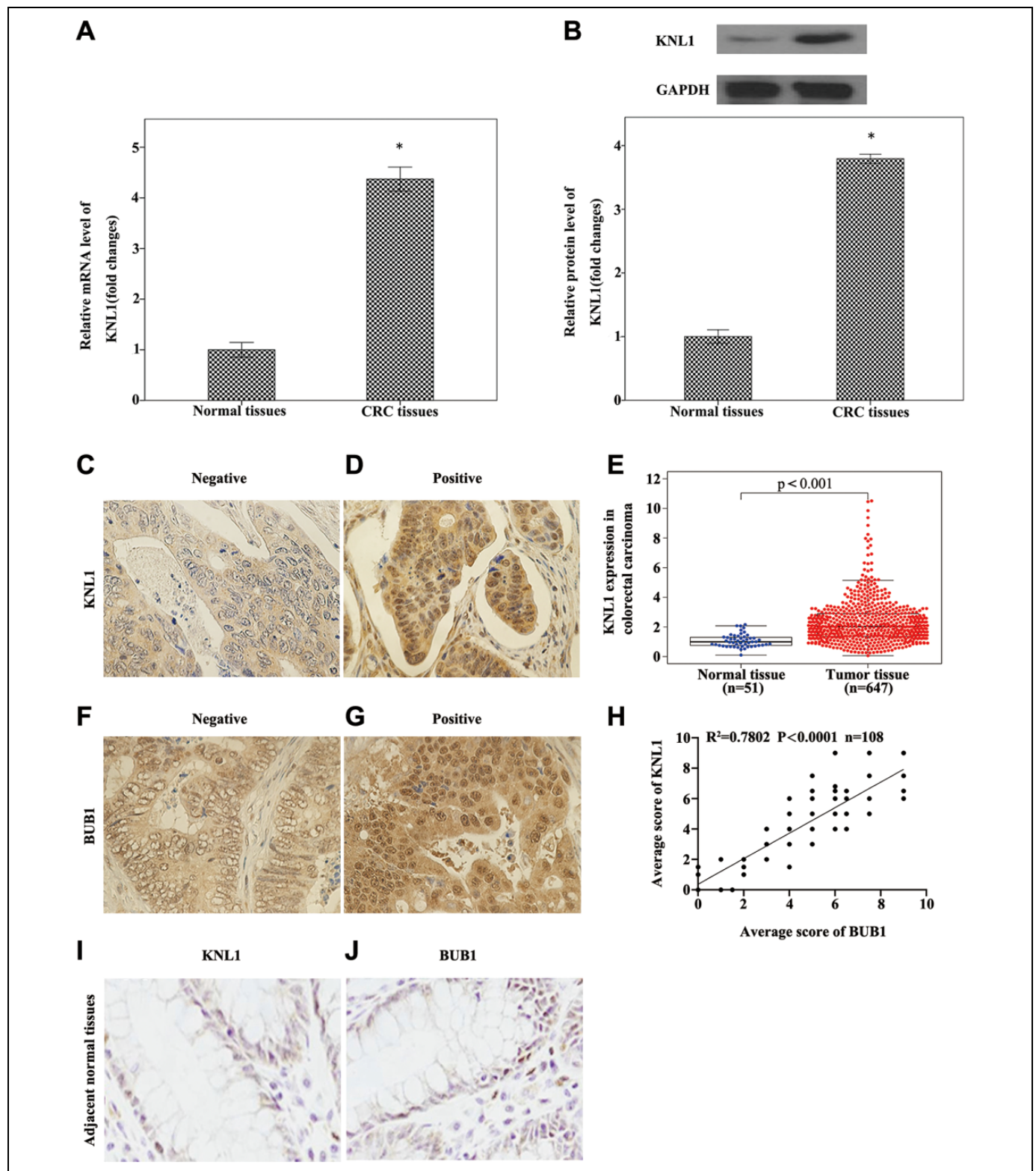


Figure 1. Expression of KNL1 in CRC and normal tissues. (A) *KNL1* mRNA expression levels in 108 paired CRC and normal adjacent tissues detected by RT-qPCR and normalized against *GAPDH*. Data analyzed by paired *t*-test ($n=3$). (B) KNL1 protein expression levels in 108 paired CRC and normal adjacent tissues detected by western blot analysis. Representative sample of KNL1 western blot band. Data analyzed by paired *t*-test ($n=3$). (C-F) Representative samples of negative and positive KNL1 and BUB1 immunostaining. Original magnification, $\times 400$. (G) KNL1 expression data obtained from The Cancer Genome Atlas website. (I and J) Representative immunostaining of KNL1 and BUB1 in adjacent normal tissues. Original magnification, $\times 400$. D and I, and G and J represent paired tissues from the same patients, respectively. $*P < 0.05$.

with tumor differentiation, but not with sex, lymph node metastasis, TNM stage, infiltration depth, age, or tumor location (Supplementary Table 1).

KNL1 expression in colorectal cancer cell lines

KNL1 mRNA and protein expression levels in SW480, RKO, HT-29, and HCT-116 CRC cells and in NCM460 normal colonic epithelial cells were determined by RT-qPCR and western blotting, respectively. Both KNL1 mRNA and protein were significantly more highly expressed in CRC compared with normal cells (all $P < 0.01$) (Figure 2A-C).

Association between KNL1 expression and survival

We created survival curves to analyze the association between KNL1 protein expression and prognosis of CRC patients. Positive expression of KNL1 was significantly associated with poorer survival ($P = 0.01$) (Figure 2D).

Lentivirus-mediated knockdown of KNL1 in CRC cells

To assess the mechanism of KNL1 in CRC, we carried out *KNL1* knockdown in RKO and HT-29 cells by transfection with a shKNL1 lentivirus. After 3 days, >80% of the cells were successfully transfected with either shCtrl or shKNL1 lentivirus (Figure 3A and B). *KNL1* mRNA expression was significantly lower in the shKNL1 compared with the shCtrl-infected cells after 5 days of transfection, as determined by RT-qPCR ($P < 0.01$) (Figure 3C and D). These results were confirmed by western blotting, indicating that the target gene was successfully knocked down (Figure 3E and F).

Inhibition of CRC cell proliferation by KNL1 knockdown

RKO and HT-29 cells transfected with shCtrl lentivirus or shKNL1 lentivirus and blank control cells were seeded into 96-well plates and analyzed using Celigo for 5 consecutive days. The numbers of cells in the shCtrl groups increased over the 5 days, whereas the numbers of cells in the shKNL1-transduced groups increased only slightly according to cell counting and MTT assays in both RKO (Figure 4A-E) and HT-29 cells (Figure 4F-J) ($P < 0.01$ at 4 and 5 days). These results suggest that *KNL1* knockdown significantly inhibited CRC cell proliferation. KNL1 expression thus appeared determine the growth of RKO and HT-29 cells.

Inhibition of CRC colony formation by KNL1 knockdown

RKO and HT-29 cells were stained with crystal violet to assess colony formation (Figure 5A and B). The number of the cells per colony was significantly higher in the shCtrl compared with the shKNL1 group (shCtrl: 229 ± 9 vs. shKNL1: 40 ± 5 ; shCtrl: 259 ± 2 vs. shKNL1: 55 ± 3 ; $P < 0.01$) (Figure 5C and D), indicating that the endogenous reduction in *KNL1* expression significantly inhibited CRC cell growth.

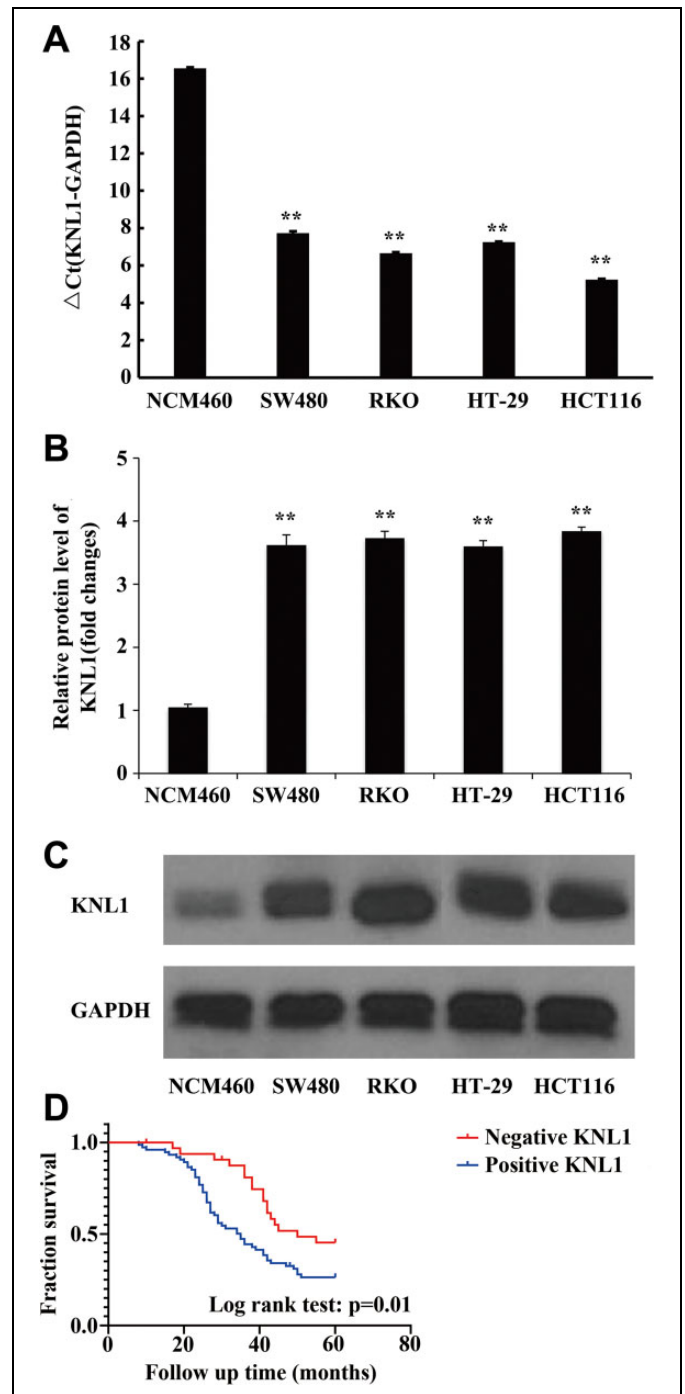


Figure 2. KNL1 mRNA and protein levels in colorectal cancer (CRC) and normal colonic epithelial cell lines. (A) KNL1 mRNA expression levels determined by RT-qPCR and (B and C) KNL1 protein expression levels determined by western blotting in CRC (SW480, RKO, HT-29, and HCT116) and normal colonic epithelial (NCM460) cell lines ($n = 3$) (** $P < 0.01$). (D) Survival curves, correlated with overall survival, in patients with positive and negative expression of KNL1 ($P = 0.01$).

Effect of KNL1 knockdown on apoptosis of RKO cells

The apoptotic rate of RKO cells was significantly higher in the shKNL1 compared with the shCtrl group ($14.86 \pm 0.30\%$ vs $4.32 \pm 0.13\%$) ($P < 0.01$) (Figure 5E and F).

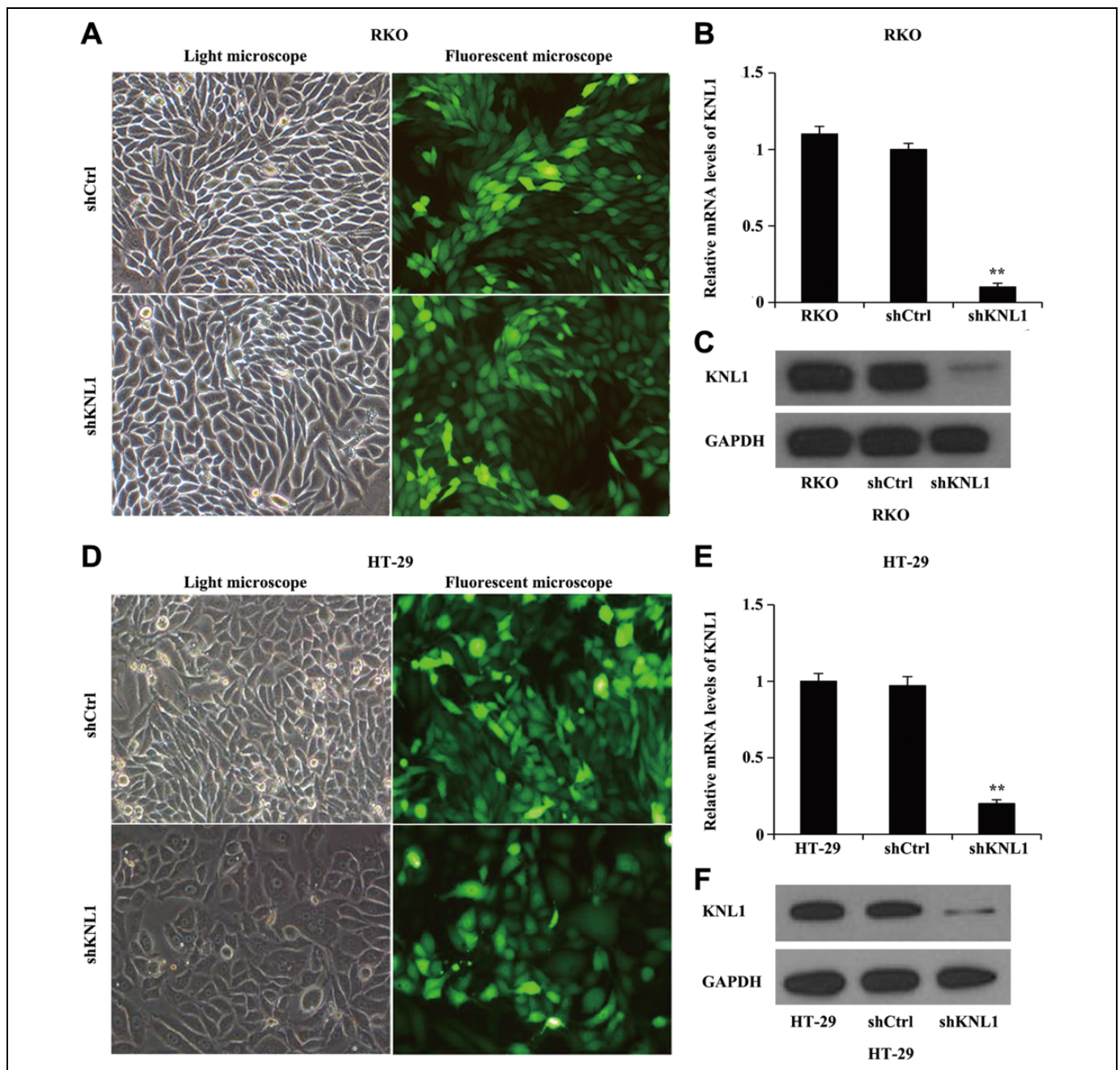


Figure 3. Knockdown of *KNL1* in RKO and HT-29 cells infected with shKNL1 or shCtrl. (A and B) Representative images of cells examined by fluorescent and light microscopy at day 3 post-infection ($\times 200$ magnification). (C and D) *KNL1* mRNA levels were analyzed by RT-qPCR at day 5 post-infection. *KNL1* mRNA levels decreased significantly after *KNL1* knockdown (** $P < 0.01$). (E and F) *KNL1* protein expression was analyzed by western blotting in transduced RKO and HT-29 cells at day 5 post-infection. *KNL1* protein levels were significantly lower in the experimental compared with the control group.

Impact of *KNL1* knockdown on cell cycle of RKO cells

DNA ploidy assay demonstrated that the proportion of G1-phase RKO cells was significantly higher in the shKNL1 compared with the negative control group ($53.05 \pm 6.71\%$ vs $35.58 \pm 5.42\%$) ($P < 0.05$) (Figure 5G and H). There were also reductions in the percentages of both S phase and G2 phase cells.

Discussion

The morbidity and mortality rates of CRC have risen rapidly, and it has therefore attracted worldwide attention.^{36,37} Despite improvements in clinical practice and treatment, outcomes of CRC patients remain poor owing to metastasis or drug resistance.^{38,39} It is therefore necessary to identify new therapeutic

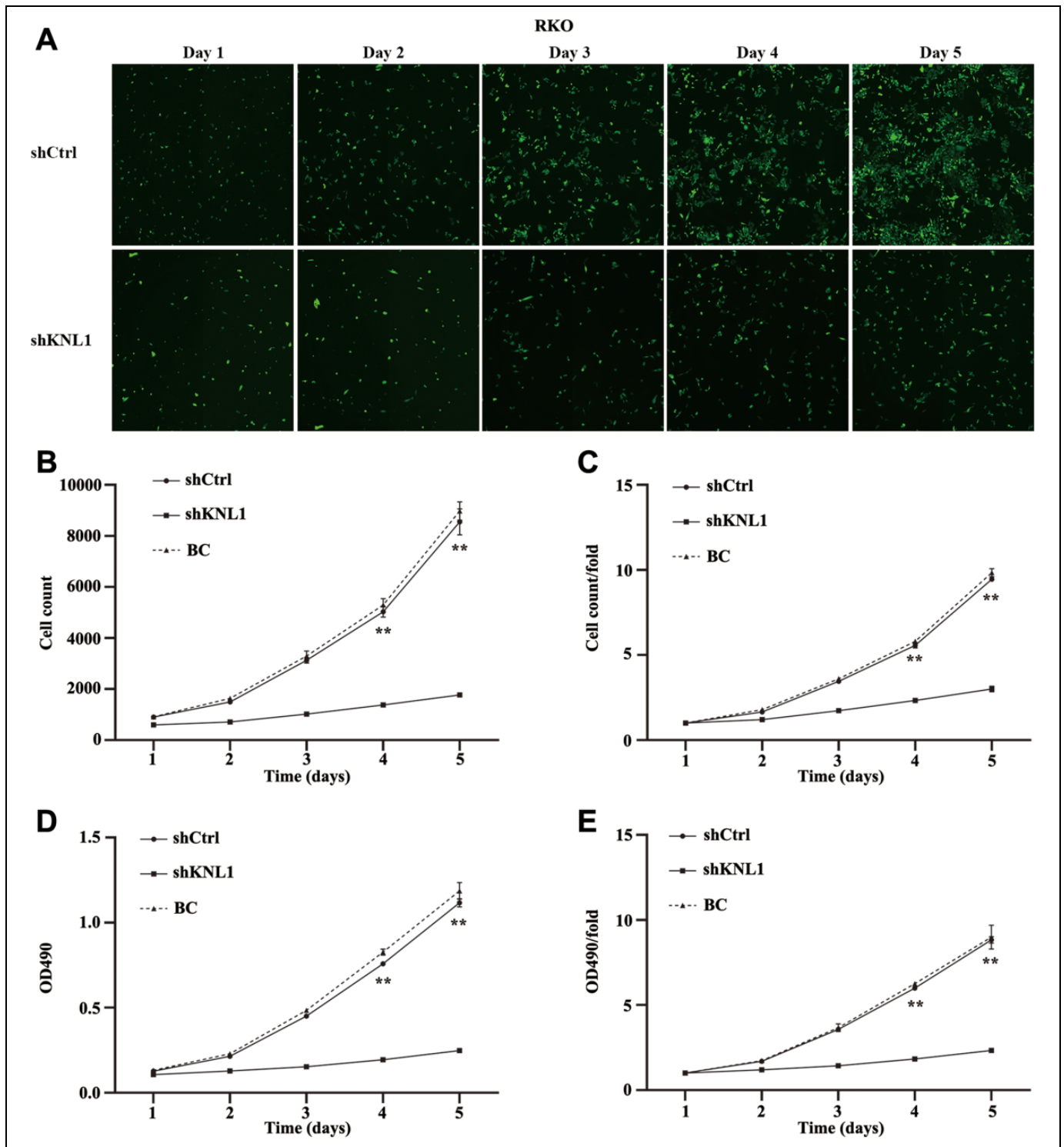


Figure 4. *KNL1* knockdown inhibited RKO cell growth. (A) Cell counts increased in time-dependent manners in RKO cells infected with shCtrl and shKNL1, respectively, for 5 days, as shown by fluorescence microscopy (green staining). Cell growth was significantly slower in the shKNL1 compared with either the shCtrl or blank control group according to (B) Celigo Cell Counting, (C) count-fold curves, and (D and E) MTT assay. *KNL1* knockdown inhibited HT-29 cell growth compared with the control group. (F) The cell count increased in a time-dependent manner in HT-29 cells infected with shCtrl and shKNL1, respectively, for 5 days, as shown by fluorescence microscopy. Cell growth was significantly slower in the shKNL1 compared with either the shCtrl or blank control group according (G) Celigo Cell Counting, (H) count-fold curves, and (I and J) MTT assay. BC, blank control. ** $P < 0.01$.

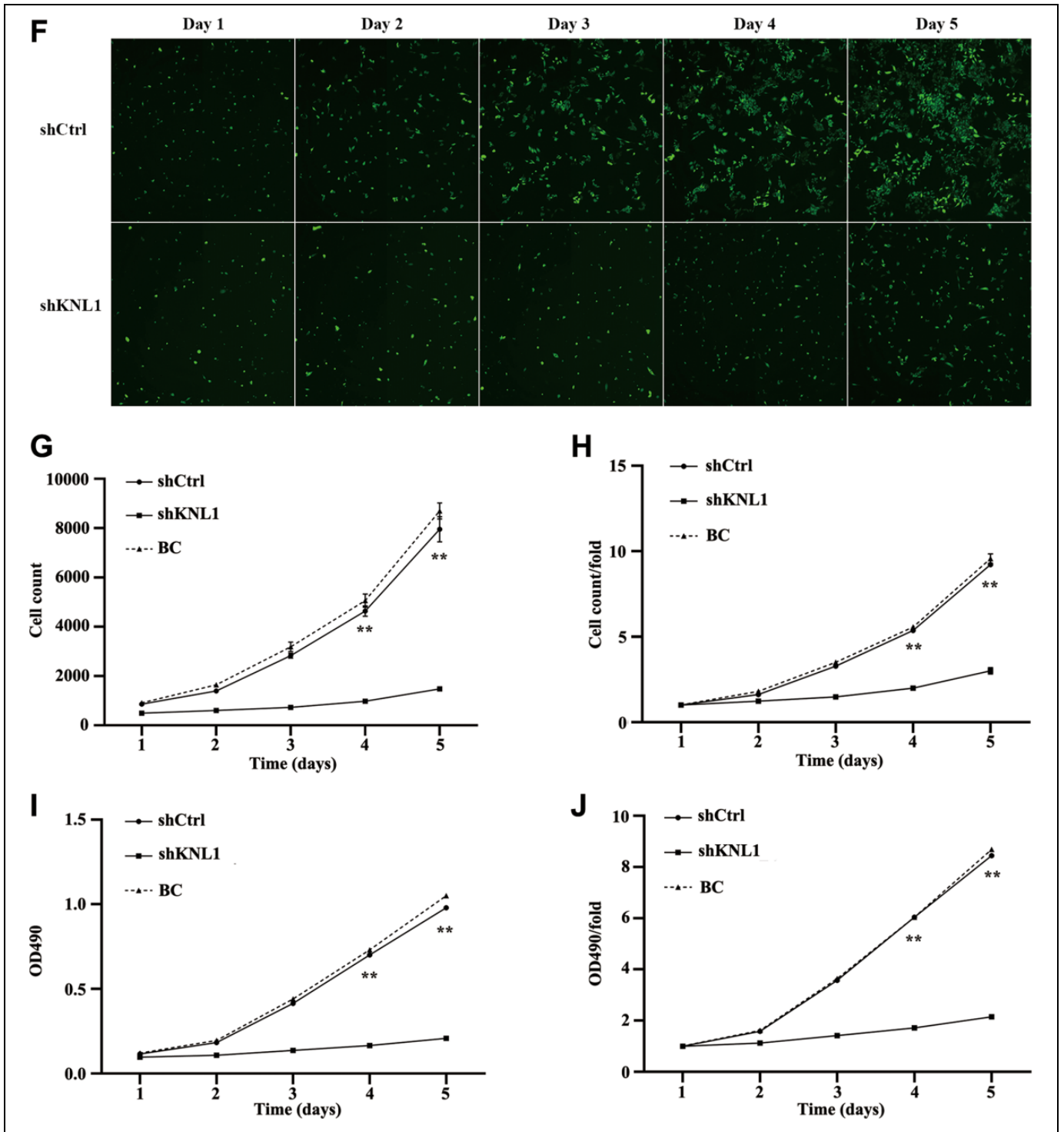


Figure 4. (continued).

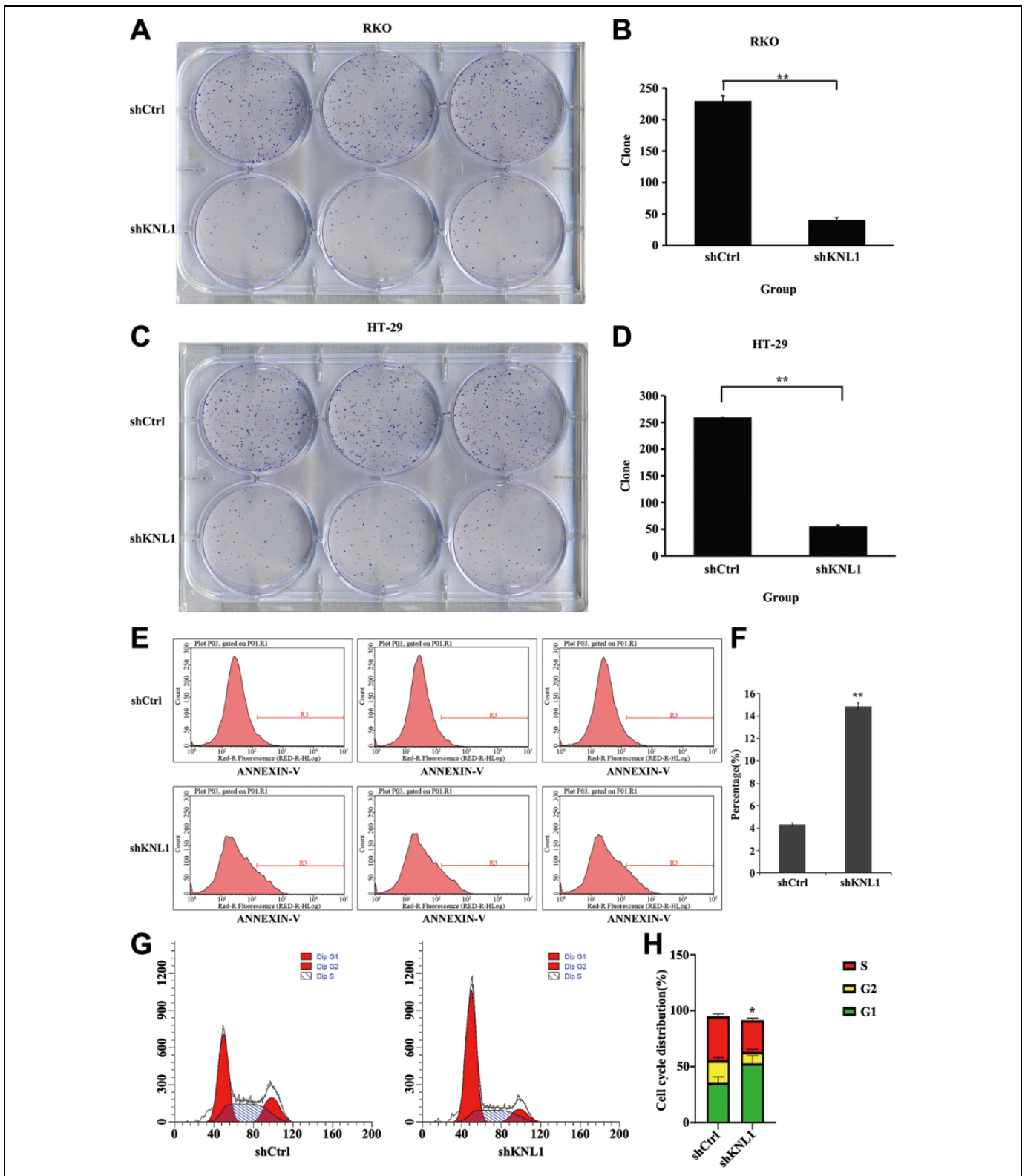


Figure 5. *KNL1* silencing repressed RKO and HT-29 cell colony formation. (A and B) Photomicrographs of crystal violet-stained colonies of RKO and HT-29 cells growing in 6-well plates at 10 days after infection. (C and D) There were significantly fewer colonies in the shKNL1-transfected RKO and HT-29 cell cultures compared with the respective control cultures. RKO cell apoptosis analyzed by flow cytometry. (E) Cells were transfected with shKNL1 and shCtrl and apoptosis was analyzed by flow cytometry. Each group is shown in triplicate. (F) Apoptosis was significantly higher in the shKNL1 compared with the shCtrl group. (G and H) Proportions of cells in various cell cycle stages, determined by flow cytometry. * $P < 0.05$; ** $P < 0.01$.

targets and to improve our understanding of the underlying molecular mechanisms.

The occurrence and development of tumors are associated with both behavioral and environmental factors, and tumorigenesis is associated with the accumulation of genetic mutations over time. Identifying the affected genes may thus aid the development of advanced diagnostic and treatment methods for cancer.

The spindle checkpoint controls mitotic progression. The human kinetochore oncoprotein AF15q14/KNL1, which belongs to the Spc105/Spc7/KNL-1 family, has been reported to provide direct links between the spindle checkpoint proteins BUB1 and BubR1 and the kinetochores, and also to play a crucial role in the alignment of chromosomes and spindle checkpoints. Previous studies^{22,27} showed that *KNL1* RNA interference resulted in accelerated mitosis due to chromosome misalignment and checkpoint failure, caused by the lack of microtubule attachment and kinetochores. Another study reported that transfection with *KNL1* small interfering RNA resulted in cancer cell apoptosis and inhibited the growth of these cells both *in vitro* and *in vivo*, regardless of p53 status.⁴⁰ However, to the best of our knowledge, no previous specific studies have reported on the role of *KNL1* expression in human cancers, particularly CRC.

The results of the present study suggest an obvious relationship between KNL1 and CRC cell apoptosis and proliferation. Although many studies have described abnormal mitosis in cancer cells treated with *KNL1* siRNA,^{22,41} the current results provide the first evidence to demonstrate that *KNL1* downregulation induced apoptosis and inhibited the growth of CRC cell lines.

However, the current study had several limitations. The number of clinical samples was relatively small and a larger sample size is required to verify the expression of KNL1 in colorectal tumors. Furthermore, there was a lack of relevant clinical information regarding patients' cause of death.

In conclusion, the results of the present study indicated that KNL1 expression was increased in CRC tissues. Furthermore, *KNL1* gene knockdown in CRC cells reduced its gene and protein expression levels, which in turn induced apoptosis and inhibited proliferation. *KNL1* knockdown may therefore be an effective therapeutic approach for the treatment of CRCs with *KNL1* overexpression.

Availability of data and materials

The datasets used and/or analyzed during the current study are available from the corresponding author on reasonable request.

Ethics approval and consent to participate

This study was approved by the Ethics Committee of the Fourth Hospital of Hebei Medical University, China. Protocol number: 120/2015, TL Bai.

Authors' Note

Tianliang Bai and Yalei Zhao contributed equally to this work.


Declaration of Conflicting Interests

The author(s) declared no potential conflicts of interest with respect to the research, authorship, and/or publication of this article.

Funding

The author(s) received no financial support for the research, authorship, and/or publication of this article.

ORCID iD

Binghui Li, PhD  <https://orcid.org/0000-0002-1791-2327>

Supplemental Material

Supplemental material for this article is available online.

References

1. Khan K, Cunningham D, Chau I. Targeting angiogenic pathways in colorectal cancer: Complexities, challenges and future directions. *Curr Drug Targets* 2017;18(1):56-71.
2. Cunningham D, Atkin W, Lenz HJ, et al. Colorectal cancer. *Lancet* 2010;375(9719):1030-1047.
3. Chen W, Zheng R, Baade PD, et al. Cancer statistics in China, 2015. *CA Cancer J Clin* 2016;66(2):115-132.
4. Siegel RL, Miller KD, Jemal A. Cancer statistics, 2016. *CA Cancer J Clin* 2016;66(1):7-30.
5. Siegel RL, Miller KD, Fedewa SA, et al. Colorectal cancer statistics, 2017. *CA Cancer J Clin* 2017;67(3):177-193.
6. Siegel RL, Miller KD, Jemal A. Cancer statistics, 2017. *CA Cancer J Clin* 2017;67(1):7-30.
7. Qian WF, Guan WX, Gao Y, et al. Inhibition of STAT3 by RNA interference suppresses angiogenesis in colorectal carcinoma. *Braz J Med Biol Res* 2011;44(12):1222-1230.
8. Wei G, Takimoto M, Yoshida I, et al. Chromosomal assignment of a novel human gene D40. *Nucleic Acids Symp Ser* 1999;(42):71-72.
9. Simpson AJ, Caballero OL, Jungbluth A, et al. Cancer/testis antigens, gametogenesis and cancer. *Nat Rev Cancer* 2005;5(8):615-625.
10. Takimoto M, Wei G, Dosaka-Akita H, et al. Frequent expression of new cancer/testis gene D40/AF15q14 in lung cancers of smokers. *Br J Cancer* 2002;86(11):1757-1762.
11. Zhao Y, Ando K, Oki E, et al. Aberrations of BUBR1 and TP53 gene mutually associated with chromosomal instability in human colorectal cancer. *Anticancer Res* 2014;34(10):5421-5427.
12. Yan M, Song M, Bai R, et al. Identification of potential therapeutic targets for colorectal cancer by bioinformatics analysis. *Oncol Lett* 2016;12(6):5092-5098.
13. Han JY, Han YK, Park GY, et al. Bub1 is required for maintaining cancer stem cells in breast cancer cell lines. *Sci Rep* 2015;5:15993.
14. Shepperd LA, Meadows JC, Sochaj AM, et al. Phosphodependent recruitment of Bub1 and Bub3 to Spc7/KNL1 by Mph1 kinase maintains the spindle checkpoint. *Curr Biol* 2012;22(10):891-899.
15. Grabsch H, Takeno S, Parsons WJ, et al. Overexpression of the mitotic checkpoint genes BUB1, BUBR1, and BUB3 in gastric cancer—association with tumour cell proliferation. *J Pathol* 2003;200(1):16-22.

16. Grabsch HI, Askham JM, Morrison EE, et al. Expression of BUB1 protein in gastric cancer correlates with the histological subtype, but not with DNA ploidy or microsatellite instability. *J Pathol* 2004;202(2):208-214.
17. Hayette S, Tigaud I, Vanier A, et al. AF15q14, a novel partner gene fused to the MLL gene in an acute myeloid leukaemia with a t(11;15)(q23;q14). *Oncogene* 2000;19(38):4446-4450.
18. Sasao T, Itoh N, Takano H, et al. The protein encoded by cancer/testis gene D40/AF15q14 is localized in spermatocytes, acrosomes of spermatids and ejaculated spermatozoa. *Reproduction* 2004;128(6):709-716.
19. Cheeseman IM, Niessen S, Anderson S, et al. A conserved protein network controls assembly of the outer kinetochore and its ability to sustain tension. *Genes Dev* 2004;18(18):2255-2268.
20. Obuse C, Iwasaki O, Kiyomitsu T, et al. A conserved Mis12 centromere complex is linked to heterochromatic HP1 and outer kinetochore protein Zwint-1. *Nat Cell Biol* 2004;6(11):1135-1141.
21. Cheeseman IM, Chappie JS, Wilson-Kubalek EM, et al. The conserved KMN network constitutes the core microtubule-binding site of the kinetochore. *Cell* 2006;127(5):983-997.
22. Kiyomitsu T, Obuse C, Yanagida M. Human Blinkin/AF15q14 is required for chromosome alignment and the mitotic checkpoint through direct interaction with Bub1 and BubR1. *Dev Cell* 2007;13(5):663-676.
23. Espeut J, Cheerambathur DK, Krenning L, et al. Microtubule binding by KNL-1 contributes to spindle checkpoint silencing at the kinetochore. *J Cell Biol* 2012;196(4):469-482.
24. Caldas GV, DeLuca JG. Knl1: Bringing order to the kinetochore. *Chromosoma* 2014;123(3):169-181.
25. Vleugel M, Tromer E, Omerzu M, et al. Arrayed BUB recruitment modules in the kinetochore scaffold KNL1 promote accurate chromosome segregation. *J Cell Biol* 2013;203(6):943-955.
26. Saurin AT. Kinase and phosphatase cross-talk at the kinetochore. *Front Cell Dev Biol* 2018;6:62.
27. Silio V, McAinsh AD, Millar JB. KNL1-Bubs and RZZ provide two separable pathways for checkpoint activation at human kinetochores. *Dev Cell* 2015;35(5):600-613.
28. Espert A, Uluocak P, Bastos RN, et al. PP2a-B56 opposes Mps1 phosphorylation of Knl1 and thereby promotes spindle assembly checkpoint silencing. *J Cell Biol* 2014;206(7):833-842.
29. Thornton GK, Woods CG. Primary microcephaly: Do all roads lead to Rome?. *Trends Genet* 2009;25(11):501-510.
30. Jamieson CR, Govaerts C, Abramowicz MJ. Primary autosomal recessive microcephaly: Homozygosity mapping of MCPH4 to chromosome 15. *Am J Hum Genet* 1999;65(5):1465-1469.
31. Genin A, Desir J, Lambert N, et al. Kinetochore KMN network gene CASC5 mutated in primary microcephaly. *Hum Mol Genet* 2012;21(24):5306-5317.
32. Subramanian A, Kuehn H, Gould J, et al. GSEA-P: A desktop application for gene set enrichment analysis. *Bioinformatics* 2007;23(23):3251-3253.
33. Livak KJ, Schmittgen TD. Analysis of relative gene expression data using real-time quantitative PCR and the 2(-Delta Delta C(T)) method. *Methods* 2001;25(4):402-408.
34. Lois C, Hong EJ, Pease S, et al. Germline transmission and tissue-specific expression of transgenes delivered by lentiviral vectors. *Science* 2002;295(5556):868-872.
35. Pan Y, Shan W, Fang H, et al. Sensitive and visible detection of apoptotic cells on annexin-v modified substrate using aminophenylboronic acid modified gold nanoparticles (APBA-GNPS) labeling. *Biosens Bioelectron* 2014;52:62-68.
36. Fearon ER, Vogelstein B. A genetic model for colorectal tumorigenesis. *Cell* 1990;61(5):759-767.
37. Jemal A, Tiwari RC, Murray T, et al. Cancer statistics, 2004. *CA Cancer J Clin* 2004;54(1):8-29.
38. DeSantis CE, Lin CC, Mariotto AB, et al. Cancer treatment and survivorship statistics, 2014. *CA Cancer J Clin* 2014;64(4):252-271.
39. de Krijger I, Mekenkamp LJ, Punt CJ, et al. MicroRNAs in colorectal cancer metastasis. *J Pathol* 2011;224(4):438-447.
40. Urata YN, Takeshita F, Tanaka H, et al. Targeted knockdown of the kinetochore protein D40/Knl-1 inhibits human cancer in a p53 status-independent manner. *Sci Rep* 2015;5:13676.
41. Krenn V, Overlack K, Primorac I, et al. KI motifs of human Knl1 enhance assembly of comprehensive spindle checkpoint complexes around melt repeats. *Curr Biol* 2014;24(1):29-39.